Spectral Analysis of High-Resolution Aeromagnetic Data for Geothermal Energy Reconnaissance across Sokoto Basin, Northwest, Nigeria

Suleiman, T.[1,2*], Okeke, F. N.[2] and Obiora, N. D.[2]

1. Ph.D. Student, Department of Science, Waziri Umaru Federal Polytechnic, Birnin Kebbi, Nigeria
2. Professor, Department of Physics and Astronomy, University of Nigeria, Nsukka, Nigeria

Abstract

This study interprets aeromagnetic data across Sokoto Basin with the aim of estimating the Curie point depth, geothermal gradient and heat flow for geothermal energy exploration. The study area lies between the longitude of 3^0E and 6^0E and latitudes 11^0N and 13^0N. The total magnetic intensity of the area was subjected to regional/residual separation using polynomial fitting. The residual data was divided into 30 overlapping spectral blocks, where the log of spectral energies was plotted against the frequency; hence, the centroid depth and the top to the magnetic sources were deduced. These depth results were used in estimating the Curie point Depth and geothermal gradient. The total magnetic intensity indicated a variation of 32932.84 to 33118.27 nT, while the residual map shows magnetic anomalies that vary from -82 to 51 nT, both maps indicated high, low and intermediary magnetic anomalies. The centroid depth results vary from 4.67 to 28.80 km, and the top to the magnetic source varies from 1.04 to 4.65 km with an average depth of 2.21 km. The Curie point depth range from 6.92 to 55.04 km with an average depth of 18.65 km, and the geothermal gradients revealed ranges from 10.54 ^{o}Ckm^{-1} at the Southwest (Danko and Gummi) areas to 83.82^{o}Ckm^{-1} at the northwest (Argungu) area. Therefore, these areas with high geothermal gradients are good indicators of geothermal energy potential and should be exploited for more power generation.

Keywords: Magnetic anomalies; Spectral Analysis; Curie Point Depth; Geothermal energy; Heat flow.

1. Introduction

Nigeria remains the largest economy in the sub-Sahara of Africa, endowed with abundant energy resources (renewable and conventional), which if properly harnessed can provide the country with sufficient capacity to meet the need of both the urban and the rural areas. Despite the abundant resources, the country has one of the lowest consumption rates of electricity per capita in Africa (i.e., far behind Cape Verde, South Africa and Ghana). This avoidable development of inadequate electricity is not only unhealthy but highly detrimental to the country's economic growth. It is alarming to note that only about 45% of the population (200 million) has access to electricity, 55% of whom are from urban areas and 45% are in rural areas (Power Africa, 2018). Nigeria, like every other country, have keyed into exploring renewable energy, thereby making efforts to provide sufficient energy that will further boost the economy. Consequently, activities are concentrated on solar energy, wind energy, and some researches are ongoing about nuclear energy as well. So far, the use of geothermal energy as an alternative source of energy has at best remains within the corridors of academics through researches in the tertiary institutions. Aeromagnetic surveys are widely used to aid in the production of geological maps and are also commonly used during mineral and geothermal exploration (Burger et al., 2006). Magnetic exploration in geothermal is important to identify the potential area of reducing magnetization due to thermal activity (Georgsson, 2009). Evaluation of geothermal potential can be done by applying the spectral analysis method to the aeromagnetic data obtained during aeromagnetic surveys. The model has proven successful in estimating average depths to the tops of magnetized bodies (Trifonova et al., 2006; Dolmaz, 2005; Tselentis, 1991). Geothermal energy is a viable and sustainable source of energy from deep inside

---

the earth, which has the potential of supplying source baseload, drive long-term energy and emission reduction of greenhouse gas (Dickson and Fanelli, 2004; Salako et al., 2020). To venture into geothermal plants in a particular area for the purpose of generating electricity, which can be of industrial usage, domestic, recreational activities, design of deep wells, oil and gas evolution history (i.e. hydrocarbon generation) there must be knowledge of the geothermal gradient of the place (Adedapo et al., 2014). Geothermal gradient is the rate of increase in temperature per unit depth in the earth due to the outflow of heat from the center (Lowrie, 1997). It indicates that heat flowing from the Earth's warm interior to its surface. On average, the temperature increases by 25°C in general for every kilometer of depth. This difference in temperature drives the flow of geothermal energy and allows humans to use this energy for heating and electricity generation. Heat flow is the flow of heat energy by conduction, convection, and radiation in sediments (Beardsmore and Cull, 2001). Heat flow from the interior to the surface of the earth is ongoing through the earth, losing its heat of planetary formation as well as the heat generated internally by radioactive decay (Hantschel and Kauerauf, 2009).

A geothermal system consists of the following: a heat sources, a reservoir, a fluid which carries and transfers heat, and a recharge area (Berktold, 1983). The heat source is due to the active tectonic plate margins, which represent major zones of magmatic matter that is cooling and radioactivity (Uysal, 2009). The reservoir of the geothermal system is the volume of rocks from which heat can be extracted. This reservoir contains hot fluids, vapor and gases. The reservoir is surrounded by colder rocks through which water flows from the outside into the reservoir. The area around the reservoir in which water (fluids) flows into the reservoir is called the recharge area. The hot fluids in the reservoir move under the influence of buoyancy forces towards a discharge area. The geothermal systems are associated with fracture and heat flow instead of specific lithology (Zira, 2013).

Depth to the bottom of magnetic sources can provide valuable information about the local and regional temperature distribution with depth and the concentration of the subsurface geothermal energy (Tselentis, 1991). Depth to the bottom of magnetic sources in a regional survey can be referred to as the Curie depth, which corresponds to a depth at which magnetic signal is lost due to the heat from the interior of the earth subsurface (Shehu et al., 2016). Estimation of curie point depth has aided in the determination of geothermal energy in different countries, as such, many authors (Bansal et al., 2010; Aboud et al., 2011; Abd & Naby, 2012; Salako and Udensi, 2013; Ofor and Udensi, 2014; Aliyu et al., 2018; Rowland and Ahmed, 2018; Adewumi et al., 2019; Salako et al., 2020) have adopted it and good results were obtained. Bhattacharyya (1966) proposed the theory for determining Curie depth, a theory which was later developed by Spector and Grant (1970). The theory shows that the Curie temperature isotherm corresponds to the temperature at which minerals lose their ferromagnetism (approximately 580°C). Thus, Curie depth isotherm corresponds to the basal surface of a magnetic crust and can be calculated from the power spectrum of the magnetic anomalies (Byerly and Stolt, 1977; Connard et al., 1983; Mishra and Naidu, 1974; Salem et al., 2000).

This investigation is therefore aimed at exploring the geothermal potential across Sokoto Basin, which can serve as an alternative to the present hydropower in the country.

2. Geology and Location of the Study Area

The study area is Sokoto Basin in Northwestern Nigeria that lies between longitudes 3^0E and 6^0E and latitudes 11^0N and 13^0N. The Basin forms the Southeastern sector of the Lullemmeden Basin, one of the young (Mesozoic–Tertiary) inland cratonic sedimentary basins of West Africa (McCurry 1976; Obaje, 2009). The Basin like other intra-continental basins and the African continent in general was developed by epeirogenic warping of stretching and rifting of technically stabilized crust. These movements commenced around the beginning of the Paleozoic and continued upper cretaceous and more responsible for the Southwestern propagation of sediments deposited within the basin (Kogbe, 1979 and

1981). In the basin, up to 2000 meters of clastic sequences rests upon the basement (Zboril, 1984). The sedimentary rocks of the basin composed of sandstone, limestone and clay of cretaceous to tertiary ages from a multilayered groundwater basin with a pumping rate of 300 liter/min at a well with 100-150 mm in diameter (Adetona and Udensi, 2007). Kogbe (1989) further described the basin as a series of crystalline massif rocks outcropping to the East and South, consisting of granite gneisses, schist, phyllites, quartzites and some amphibolite, diorite, gabbro and marble of pre-Cambrian age. The lowlands and plains of the basement areas are sometimes covered on the surface by Quaternary sediments of Aeolian and fluvial origin especially along the flood plains of the major rivers and streams. Offodile (2002) added that the basement complex occupies about 42% area of the Sokoto basin. Figure 1 shows the geological map of the study area.

3. Materials and Method
3-1. Materials
Fifteen aeromagnetic data sheets were used in estimating the geothermal potential of the study area, which were acquired from the Nigerian Geological Survey Agency (NGSA). The survey was carried out between 2005 and 2009, with terrain clearance of 80 m, line spacing of 500 m, a nominal tie-line spacing of 2 km and flight line and tie-line trends of 135 and 45° respectively. All grid data were saved and delivered in Oasis Montaj Geosoft gdb format. Each 1:100,000 topographical sheet covers an area of about 3025 km^2 (i.e. 55 x 55 km^2), therefore, this investigation is covering a total area of 45,375 km^2.
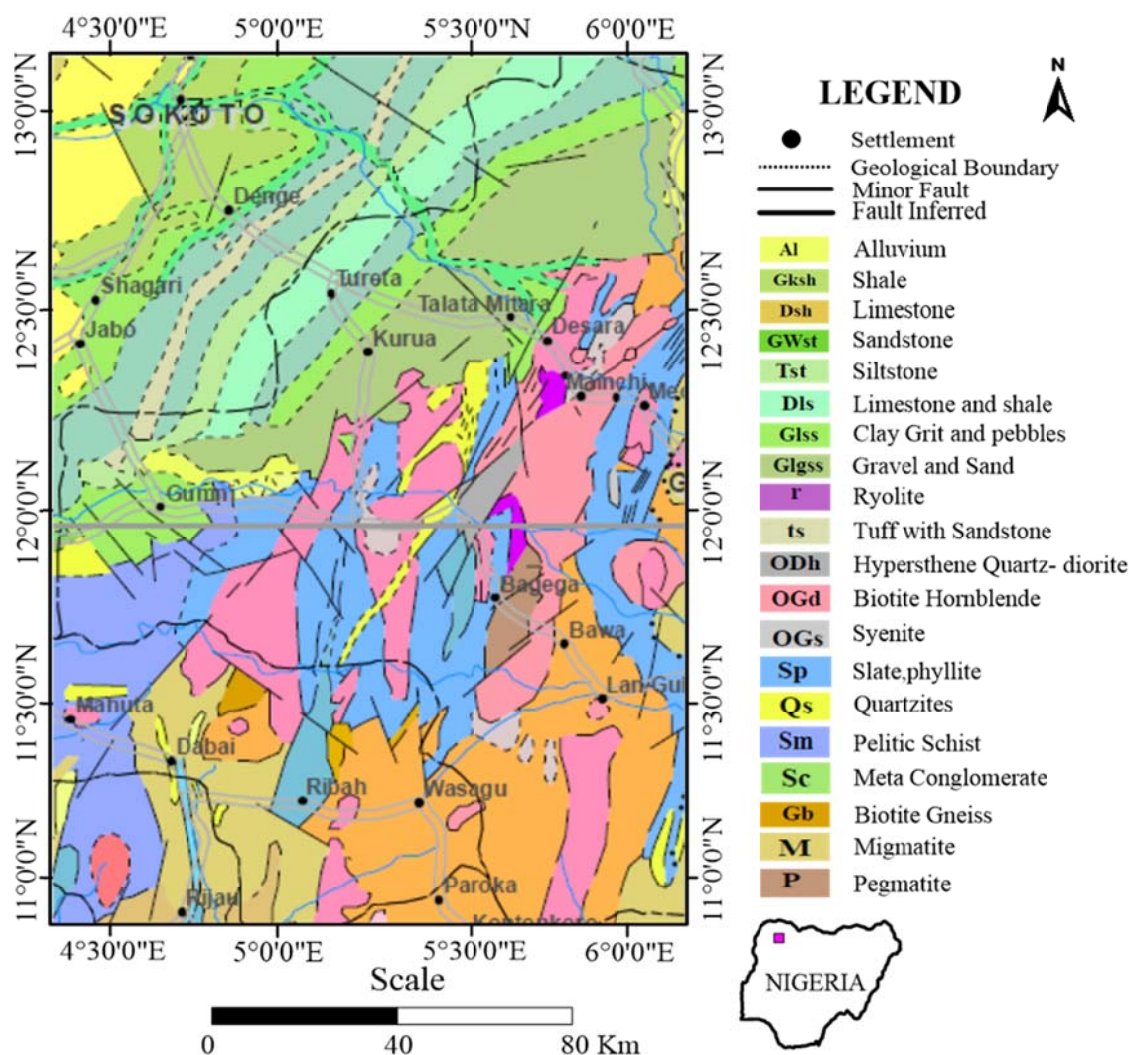

Figure 1. Geological map of the study area (After NGSA, 2009).

3-2. Methods

In actualizing the aim of this investigation, these processes were adopted, thus, reduction of the total magnetic intensity to the magnetic equator, hence, separation of regional and residual data, estimation of spectral analysis, curie point depth, geothermal gradient and heat flow.

The fifteen aeromagnetic sheets were assembled in Oasis Montaj 8.4.2v software, merged, and gridded using a bi-directional line gridding method to produce the total magnetic intensity map, TMI (Figure 2) of the area.

3-2-1. Reduction to Magnetic Equator (RTE)

Reduction to the equator is used in low magnetic latitudes to center the peak of magnetic anomalies over their sources, enhancing basement architecture including structural lineaments with its orientations thereby making the data easier to interpret without losing any geophysical meaning (Gilbert and Geldano, 1985). The TMI was reduced-to-equator in agreement with the International Geomagnetic Reference Field (IGRF) reduction technique using geomagnetic inclination angle -1.4°, geomagnetic declination angle -1.7° and a standard deviation of 0.1. Equation (1) is the expression for RTE (Leu, 1981).

$$L(\theta) = \frac{\left[\sin(I) - i.\cos(I).\cos(D-\theta)\right]^2 \times}{\left[\sin^2(Ia) + \cos^2(Ia).\cos^2(D-\theta)\right] \times} \frac{(-\cos^2(D-\theta))}{\left[\sin^2(I) + \cos^2(I).\cos^2(D-\theta)\right]} \tag{1}$$

If (/Ia/</I/), Ia = I

where I = geomagnetic inclination Ia = Inclination for amplitude correction (never less than I), D = geomagnetic declination, $L(\theta)$ is Reduction to Equator, θ is the wave number direction.

3-2-2. Regional/Residual Separation

The residual magnetic field of the study area was produced by subtracting the regional field from the total magnetic field using the polynomial fitting of second-order of least square method. Equation (2) was used in generating the algorithm for removal of regional data (Ugwu et al., 2013):

$$r = a_0 + a_1\left(x - x_{ref}\right) + a_2\left(y - y_{ref}\right) \tag{2}$$

where r is the regional field, x_{ref} and y_{ref} are the x and y coordinates of the geographic center of the data set respectively; a_0, a_1 and a_2 are the regional polynomial coefficients.

3-2-3. Spectral Method

Spectral method permits an estimation of depth of magnetized blocks of varying depth, width, thickness and magnetization (Bhattacharyya, 1966; Spector and Grant, 1970; Shuey et al., 1977; Onuoha et al., 1994; Tanaka et al., 1999). The residual data was divided into thirty window spectral blocks (block A – DD) such that, block A – O have spectral probe of 55 km by 55 km, block P – Y have spectral probe of 82.5 km by 55 km, block Z – CC have spectral probe of 165 km by 110 km and block DD has a spectral probe of 165 km by 165 km. Subsequently, spectral program plot (SPP) developed with MATLAB software was employed in the estimation of the depth to the centroid (Z_o) of the magnetic from the slope of the first-longest wavelength part of the spectrum using Equation (3) (Bhattacharyya & Leu, 1975; Okubo et al., 1985).

$$\ln\left[\frac{\sqrt{P_{(s)}}}{|s|}\right] = \ln A - 2\pi|s|Zo \tag{3}$$

where $P(s)$ is the radially averaged power spectrum of the anomaly, $|s|$ is the wavenumber, and A is constant.

Similarly, the depth to the top boundary (Z_t) was also estimated from the slope of the second-longest wavelength part of the spectrum using Equation (4) (Okubo et al., 1985).

$$\ln\left[\sqrt{P_{(S)}}\right] = \ln B - 2\pi|S|Zt \tag{4}$$

where B, is the sum of constant independent of $|s|$.

3-2-4. Curie Point Depth Estimation

The estimation of the Curie point depth (Z_b),

which is also called the basal depth was done using Equation (5) (Bhattacharyya & Leu, 1975; Okubo et al., 1985).

$$Z_b = 2Z_0 - Z_t \qquad (5)$$

where Z_0 is the centroid depth, Z_t is the depth to the top boundary and Z_b is the Curie point depth.

3-2-5. Geothermal Gradient and Heat Flow

The basic relation for conductive heat transport is Fourier's law. In a one-dimensional case under the assumption that the direction of temperature variation is vertical and the temperature gradient $\dfrac{dT}{dz}$ is constant, Fourier's law takes the form shown in Equation (6).

$$q_z = k\frac{dT}{dz} \qquad (6)$$

where q_z is heat flow and k is the thermal conductivity.

Curie temperature (θ) can be estimated from the expression in Equation (7) (Tanaka et al., 1999):

$$\theta = \frac{dT}{dz} Z_b \qquad (7)$$

Hence,

$$\frac{dT}{dz} = \frac{\theta}{Z_b} \qquad (8)$$

Equations (6) and (8) were used in computing heat flow and geothermal gradients respectively. In computing the geothermal gradient of the area, possible Curie point temperature of 580°C was used (i.e. Curie temperature of magnetite), and thermal conductivity of 2.5 $Wm^{-1o}C^{-1}$ was used (Stacey, 1977; Tanaka et al., 1999; Stampolidis et al., 2005; Nwankwo et al., 2011; Salako et al., 2020).

4. Results and Discussion
4-1. Total Magnetic Intensity, Reduction to Equator and Residual Maps

The TMI of the area shown in Figure 2 revealed that the area is magnetically heterogeneous in nature. It indicated that

magnetic intensities range between 32932.8 and 33102.5 nT, with variations of lows, highs, and intermediary magnetic signatures. The low magnetic intensities (denoted with Low) are areas associated with the sedimentary region, and are found within the North (Binji, Sokoto and Dange areas), and some intrusion of the low magnetic intensities are seen in the Southern (Zuru and Wasagu) areas. The high magnetic intensities which are probably attributes of igneous intrusion (denoted with High) are found majorly around the Southern part, which is Danko, Gwashi. Zuru and Wasagu areas. Another feature (yellow) that dominates the study area is intermediate, which corresponds to granitic rocks.
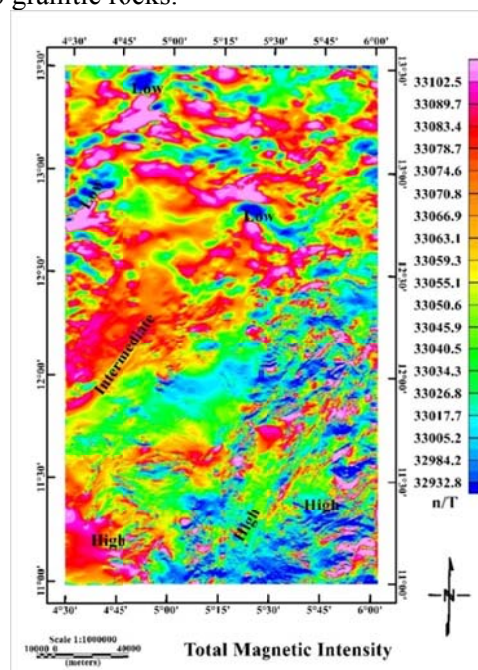

Figure 2. Total Magnetic Intensity.

Figures 3a and 3b are the maps of the reduction to the equator and the residual map of the study area respectively. The RTE and the residual maps indicated high magnetic intensities, which vary from 96 to 126 nT and 32 to 51 nT, respectively, mostly around the Southern parts. The Northern parts of the study area are dominated by rocks with low magnetic intensities of range between -45 and 13 nT for RTE and -82 to -14 nT for the residual map. The values observed are factors of the rock types present in the region and the mineral composition of the various rocks. These rocks are mostly sandstone clay and shale, pegmatite, biotite, quartzite, schist, gneiss, granite.
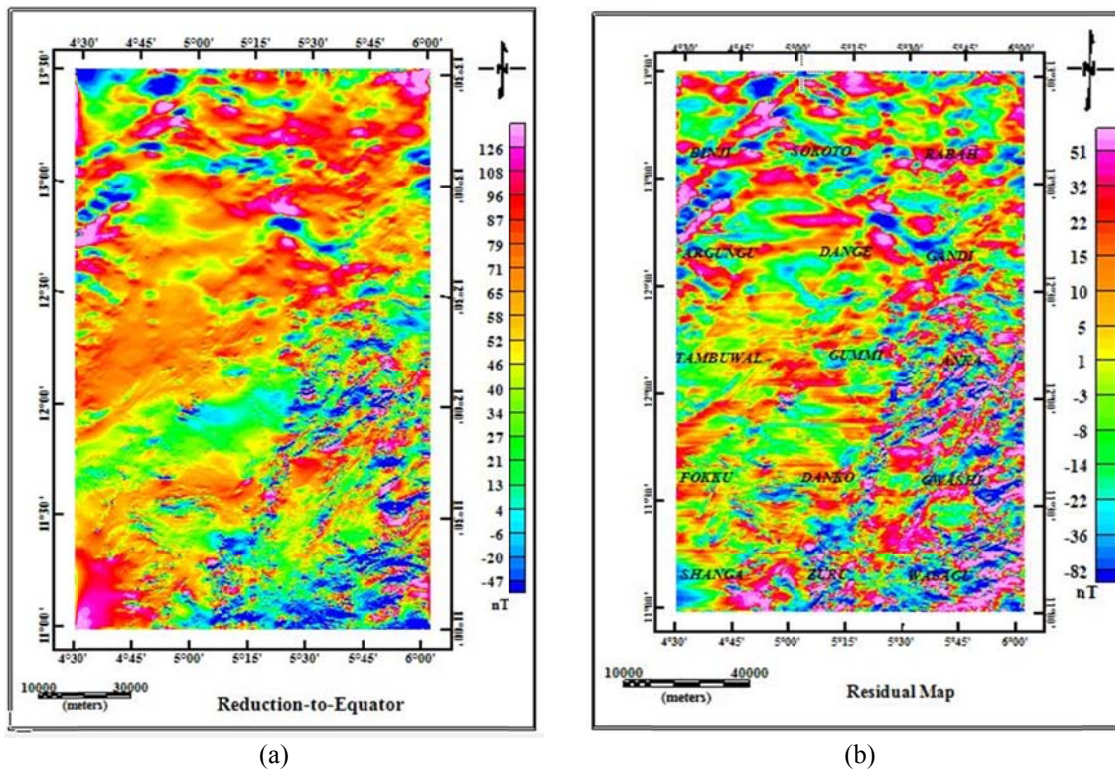
Figure 3. a) Reduction to Equator Map, b) Residual Maps.

4-2. Spectral Analysis, Curie Point Depth, Geothermal Gradient and Heat Flow

Table 1 shows block divisions, coordinates of each block, depth to the centroid (Z_o), depth to the top boundary (Z_t), CPD, geothermal gradient and heat flow.

Table 1. Results of Spectral analysis, CPD, Geothermal gradient and Heat flow.

Block	Longitude (Deg)	Latitude (Deg)	Depth to Centroid Z_o (Km)	Depth to top Z_t (Km)	Curie Point Depth Z_b (Km)	Geothermal Gradient ($^0C/Km$)	Heat Flow ($mW/m2$)
A	4.525	13.250	7.93	3.40	12.46	46.55	116.37
B	5.025	13.250	7.21	1.82	12.60	46.03	115.08
C	5.525	13.250	7.79	1.62	13.96	41.55	103.87
D	4.525	12.525	4.67	2.42	6.92	83.82	209.54
E	5.250	12.525	5.70	3.31	8.09	71.69	179.23
F	5.525	12.525	5.13	2.32	7.94	73.05	182.62
G	4.525	12.025	7.69	2.06	13.32	43.54	108.86
H	5.250	12.525	7.16	1.22	13.10	44.27	110.69
I	5.525	12.525	4.50	1.04	7.96	72.86	182.16
J	4.525	11.525	6.00	1.75	10.26	56.59	141.46
K	5.525	11.525	9.49	1.20	17.78	32.62	81.55
L	5.525	11.525	4.87	1.04	8.70	66.67	166.67
M	4.525	11.025	12.20	1.26	23.14	25.06	62.66
N	5.025	11.025	10.30	1.38	19.22	30.18	75.44
O	5.525	11.025	6.04	1.74	10.34	56.09	140.23
P	4.538	13.025	7.50	3.33	11.67	49.70	124.25
Q	5.513	13.025	6.91	1.83	11.99	48.37	120.93
R	4.538	12.525	13.50	2.57	24.43	23.74	59.35
S	5.513	13.025	9.40	3.16	15.64	37.08	92.71
T	4.538	12.025	10.70	4.65	16.75	34.63	86.57
U	5.513	12.025	8.81	2.03	15.59	37.20	93.01
V	4.538	11.525	9.68	2.70	16.66	34.81	87.03
W	5.513	11.525	6.91	1.36	12.46	46.55	116.37
X	4.538	11.025	9.57	1.89	17.25	33.62	84.06
Y	5.513	11.025	7.39	1.42	13.36	43.41	108.53
Z	5.025	12.550	14.40	3.10	25.70	22.57	56.42
AA	5.025	12.500	20.60	2.58	38.62	15.02	37.55
BB	5.025	11.550	25.00	2.26	47.74	12.15	30.37
CC	5.025	11.500	27.00	3.17	50.83	11.41	28.53
DD	5.025	12.025	28.8	2.56	55.04	10.54	26.34
Average			**10.43**	**2.21**	**18.65**	**41.71**	**104.28**

Figure 4 highlighted some selected samples of the slopes of plots of the logarithms of the spectral energies against frequency for the estimation of Z_o and Z_t. The centroid depths range from 4.67 to 28.80 km with an average of 10.43 km, while the depths to the top of magnetic sources vary from 1.04 to 4.65 km with an average depth of 2.21 km. From the depth to the top of magnetic sources, the maximum depths are observed around the Northern parts (Binji and Dange) of the area, these areas correspond with areas of low magnetic intensities as identified in the TMI. The minimum depths are observed around the Southeastern parts (Shanga and Wasagu), which correspond to the areas of high magnetic intensities. Figure 5a and 5b represent the contour map and 3D map of the depth to the top boundary (Z_t) respectively indicating the areas with maximum and minimum depths. The average depth (sedimentary thickness) obtained in this study is in close agreement with the results of Kamba et al. (2017), Bonde et al. (2014) and Nnaemeka (2017) who have carried out geophysical investigation in the basin.

Wright et al. (1985) argued that the minimum thickness of sediment required to achieve a threshold temperature for the commencement of hydrocarbon formation is 2.3 km. An average depth of 2.21 km obtained in the present study may not be considered too favorable for hydrocarbon exploration in the basin.
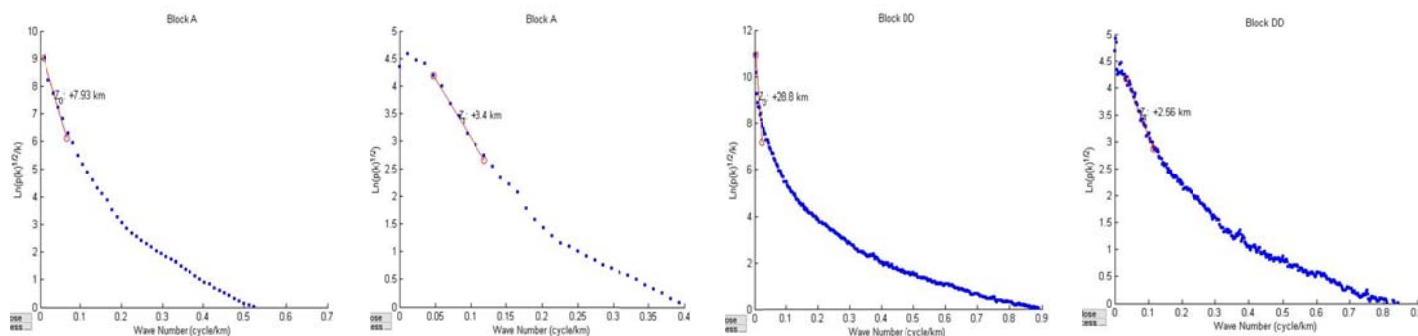

Figure 4. Sample plots of Log of Energy against Frequency.

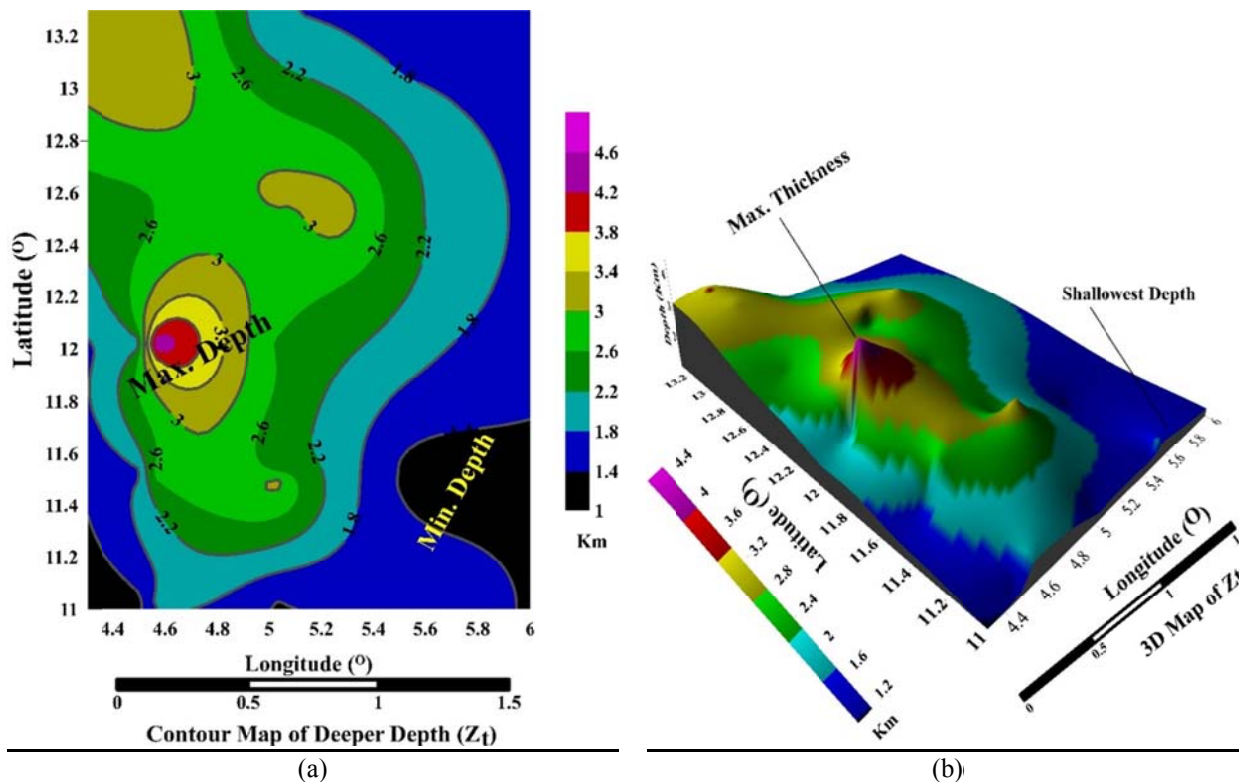(a)   (b)

Figure 5. a) 2D Contour map of the Deeper depth, b) 3D map of the deeper depth.

The CPD estimated (in accordance with Equation 5) vary between 6.92 and 55.04 km with an average value of 18.65 km. Figure 6a and 6b are the 2D contour map and the 3D view of the CPD, respectively. From the maps, it was observed that maximum depths are around the Southwest (Tambuwal and Gummi areas) towards the Northern parts, while the minimum depths are in the Southeastern parts towards the Northeast. The low values observed in this study may be attributed to igneous intrusion or dominance of sandstone in the area. Results of CPD are greatly dependent on the geologic conditions and mineralogical contents of an area, they are shallower in the volcanic and geothermal field (Bhattacharyya and Leu, 1975; Tanaka et al., 1999; Eletta and Udensi, 2012; Aliyu et al., 2018). Therefore, it may be inferred that the areas with shallower depths are

hotspots for geothermal energy.

Results from the estimated geothermal gradient (Figure 7) (using Equation 8) revealed a minimum of 10.54 ^{O}Ckm^{-1} to a maximum of 83.82 ^{O}Ckm^{-1} with an average of 41.71 ^{O}Ckm^{-1} in the study area. Similarly, the heat flow values (using Equation 6) ranged from 26.34 mWm^{-2} to 209.54 mWm^{-2} with an average value of 104.28 mWm^{-2} (Figure 8). The maximum geothermal gradients are observed around the Northwest (Argungu) and the Northeastern parts (Gandi and Rabah), these areas fall within the Sokoto river of the inland sedimentary basin with possibility of igneous intrusion that provides for appropriate geothermal energy. These results are compared favorably with the results of other researchers (Ofor and Udensi, 2014; Shehu et al., 2016) within the basin.
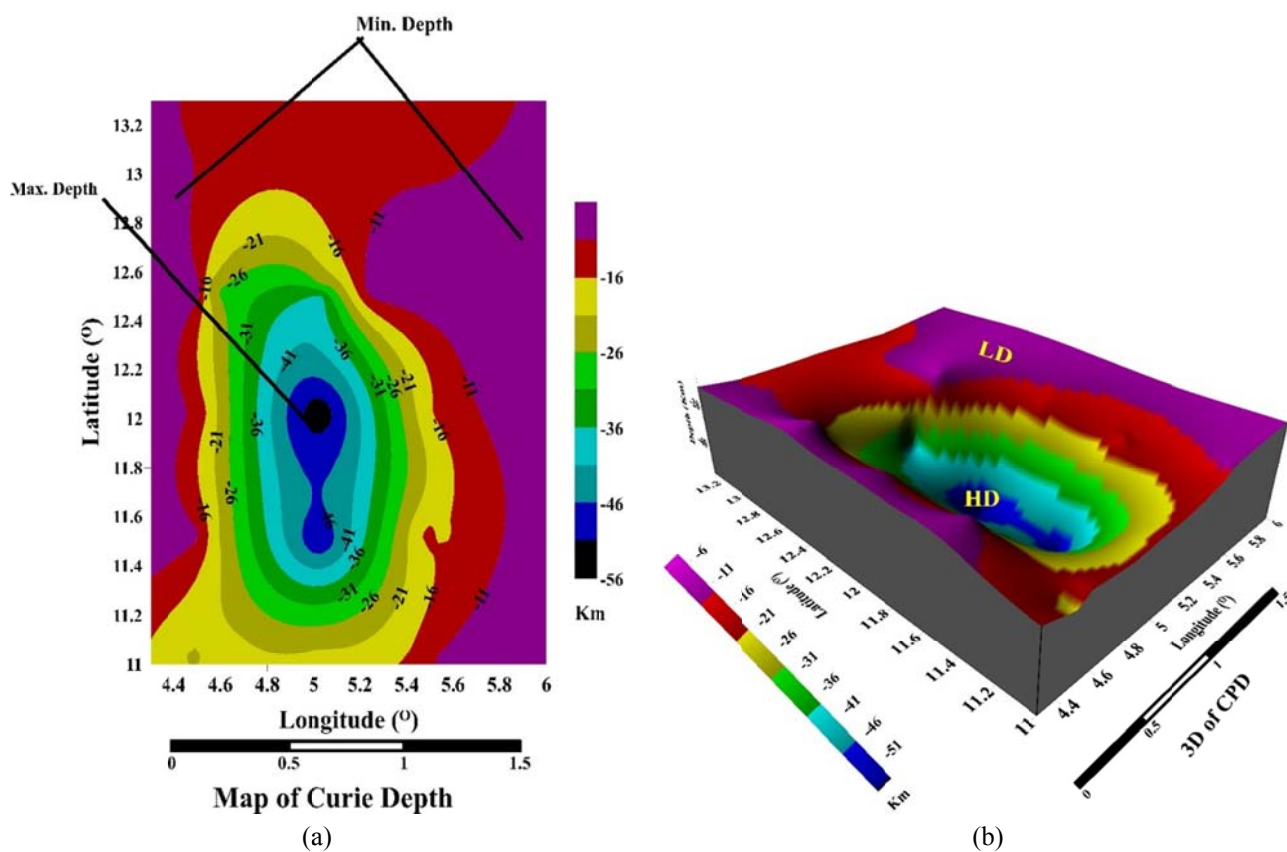

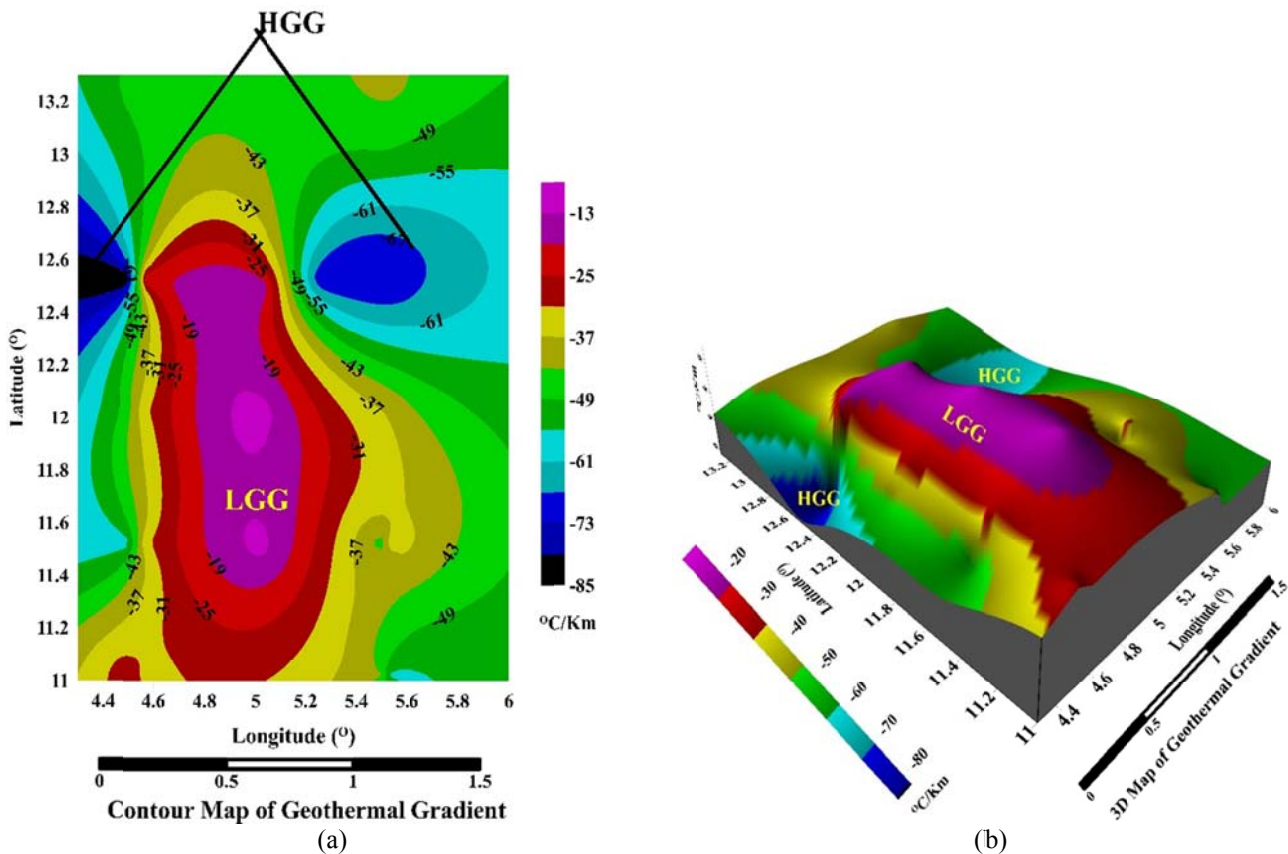**Figure 6.** a) 2D Contour Map of CPD, b) 3D View of CPD.

Figure 7. a) 2D Contour Map of Geothermal Gradient, b) 3D View of Geothermal Gradient.
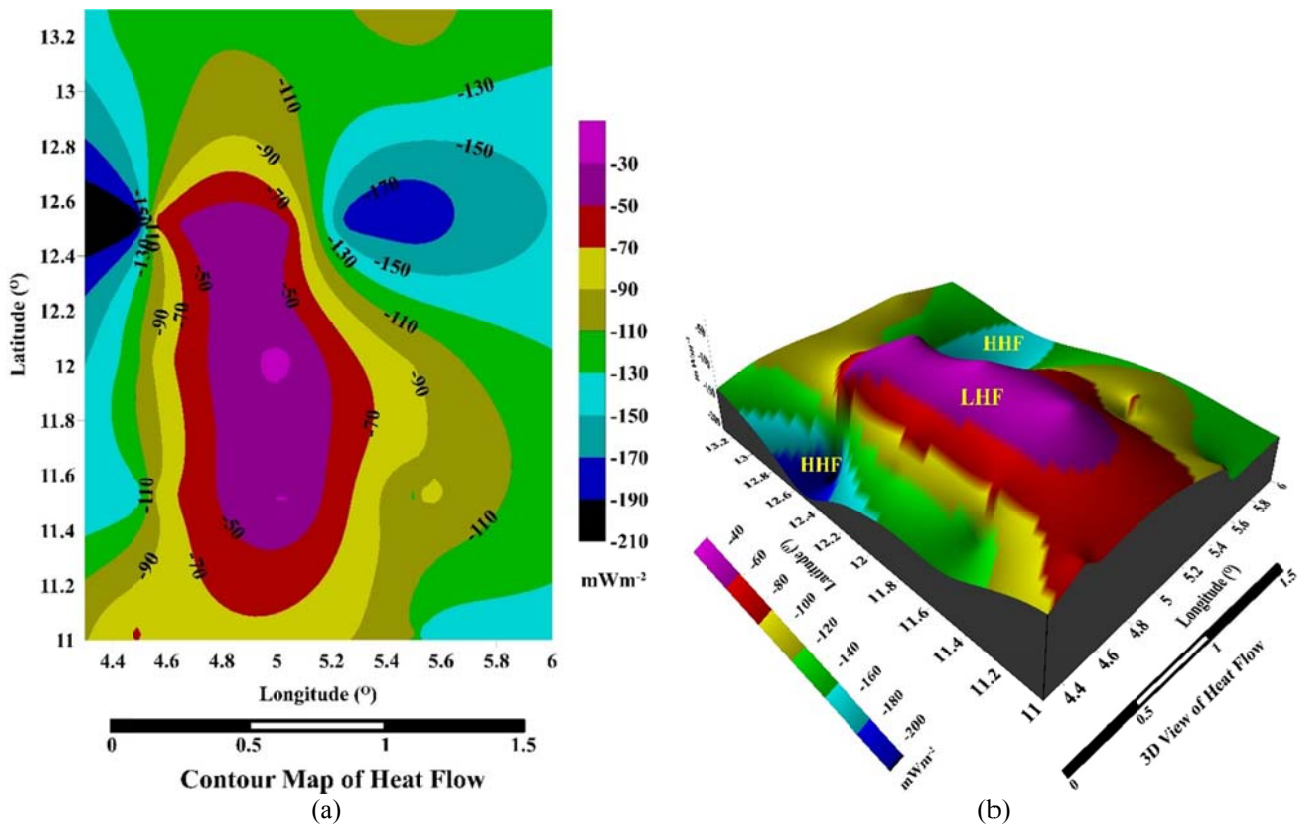

Figure 8. a) Contour Map of Heat Flow, b) 3D View of Heat Flow.

5. Conclusion

An investigation of the geothermal energy potential across Sokoto Basin was carried out using high-resolution aeromagnetic data and the results show that the Northwest (Argungu) and Northeastern parts (Gandi and Rabah) of the areas have high potentials because they are associated with shallower Curie point, high geothermal gradient and high heat flow. Hence, exploiting the geothermal prospect of these areas with high geothermal gradients will go a long way in adding to the power generation in Nigeria. These results have no doubt provided important geophysical inputs, which are useful for geothermal exploration in the basin.

References

Abd, E.L. and Nabi, S.H., 2012, Curie point depth beneath the Barramiya-Red Sea coast area estimated from aeromagnetic spectral analysis. J. Asian Earth Sci., 43, 254–266.

Aboud, A., Salem, A. and Mekkawi, M., 2011, Curie depth map for Sinai Peninsula, Egypt deduced from the analysis of magnetic data. Tectonophysics, 506, 46–54.

Adedapo, J.O., Ikpokonte, A.E., Kurowska, E. and Schoeneich, K., 2014, An Estimate of Oil Window in Nigeria Niger Delta Basin from Recent Studies. Am. Int. J. Cont. Res., 4(9), 114-121.

Adetona, A.A. and Udensi, E.E., 2007, Spectral Depth Determination to Buried Magnetic Rocks under the Lower Sokoto basing using aeromagnetic Data. Nigeria Journal of Physics (NIP), 19(2), 275-283.

Adewumi, T., Salako, K.A., Adediran, O.S., Okwoko, O.I. and Sanusi, Y.A., 2019, Curie point Depth and Heat Flow Analyses over Part of Bida Basin, North Central Nigeria using Aeromagnetic Data. Journal of Earth Energy Engineering, 8(1), 1-8.

Aliyu, A., Salako, K.A., Adewumi, T. and Mohammed, A., 2018, Interpretation of High-Resolution Aeromagnetic Data to Estimate the Curie Point Depth Isotherm of Parts of Middle Benue Trough, North-East, Nigeria. Physical Science International Journal, 17(3), 1-9.

Bansal, A., Gabriel, G. and Dimri, V., 2010,

Depth to the bottom of magnetic sources in Germany. EGM 2010 International Workshop Adding new value to Electromagnetic, Gravity and Magnetic Methods for Exploration Capri, Italy.

Beardsmore, G.R. and Cull, J.P., 2001, Crustal heat flow: A guide to measurement and modeling. Cambridge University Press, New York, pg. 332.

Berktold, A., 1983, Electromagnetic studies in geothermal regions: Geophys. Surv., 6, 173-200.

Bhattacharyya, B.K., 1966, Continuous spectrum of the total magnetic field anomaly due to a rectangular prismatic body. Geophysics, 31, 97:121. 21.

Bhattacharyya, B.K. and Leu, L.K., 1975, Analysis of magnetic anomalies over Yellowstone National Park: Mapping of Curie point isothermal surface for geothermal reconnaissance. Journal of Geophysical Research, 80, 4461–4465.

Bonde, D.S., Udensi, E.E. and Momoh, M., 2014, Modeling of Magnetic Anomaly zones in Sokoto Basin, Nigeria. IOSR Journal of Applied Geology and Geophysics, 2(1), Ver. I. PP 19-25.

Byerly, P. and Stolt, R.H., 1977, An attempt to define the Curie Point Isotherm in Northern and Central Arizona, Geophysics, 42, 1394-1400.

Connard, G., Couch, R. and Gempererie, M., 1983, Analysis of Aeromagnetic measurement from the Cascade Range in Central Oregon, Geophysics, 48, 376-390.

Dickson, M. and Fanelli, M., 2004, What is geothermal energy. Instituto di Geoscienze e Georisorse, CNR , Pisa, Italy.

Dolmaz, M.N., Ustaomer, T., Hisarli, Z.M. and Orbay, N., 2005, Curie point depth variations to infer thermal structure of the crust at the African-Eurasian convergence zone, SW Turkey. Earth Planets Space, 57, 373–383.

Eletta, B.E. and Udensi, E.E., 2012, Investigation of Curie point isotherm from the magnetic field of Easter sector of central Nigeria. Global journal of Geosciences, 101– 106.

Georgsson, L.S., 2009, Geophysical methods in geothermal exploration. Short Course on Surface Exploration for Geothermal Resources, UNU-GTP and La Geo, El

Salvador.

Gilbert, D. and Geldano, A., 1985, A computer programme to perform transformations of gravimetric and aeromagnetic surveys. Comput. Geosci., 11, 553–588.

Hantschel, T. and Kauerauf, A.A., 2009, Fundamentals of Basin and Petroleum Systems Modeling. Spring-Verlag Berlin Heidelberg.

Kamba, A.H., Muhammad, S. and Illo, A.G., 2017, Basement Depth Estimates of some part of Lower Sokoto Sedimentary Basin, North-western Nigeria, Using Spectral Depth Analysis. International Journal of Marine, Atmospheric & Earth Sciences, 6(1), 1-9.

Kogbe, C.A., 1989, Cretaceous and Tertiary of the Iullemmeden Basin in Nigeria in: C.A. Kogbe (eds.), Geology of Nigeria, 377-421. Jos, Rock View Publ. Co.

Kogbe, C.A., 1979, Geology of the South Eastern (Sokoto) Sector of the Iullemmeden Basin Bulletin, Department of Geology, Ahmadu Bello University, Zaria, Nigeria. 2(1), 2.

Kogbe, C.A., 1981, Cretaceous and Tertiary of the Iullemmeden Basin in Nigeria (West Africa) Cretaceous Research, 2, 129-186.

Leu, L.K., 1981, Use of reduction-to-equator process for magnetic data interpretation: Presented at the 51st Ann, Internat. Mtg., Sot. Exnl. Geonhv, Geophysics, 47, 445.

Lowrie, W., 1997, Fundamental of Geophysics. Cambridge University Press, United Kingdom.

McCurry, P., 1976, The geology of the Precambrian to lower paleaozoic rocks of Northern Nigeria: A Review. In Kogbe CA, (ed.), Geology of Nigeria. Lagos: Elizabethan Pub. Co. 18-40.

Mishra, D.C. and Naidu, P.S., 1974, Two-dimensional Power spectral analysis of aeromagnetic Fields. Geophysics Prop, 22, 345–534.

Nnaemeka, E.B., 2017, Geophysical Investigation of Argungu and Dange areas, Sokoto Basin Nigeria using aeromagnetic data. Unpublished M.Sc. Thesis, University of Nigeria, Nsukka, Enugu, Nigeria. Pp. 81.

Nwankwo, L.I., Olasehinde, P.I. and Akoshile, C.O., 2011, Heat flow anomalies from spectral analysis of aeromagnetic data of Nupe Basin, Nigeria. Asian Journal of Earth Sciences. 1–7.

Obaje, N.G., 2009, Geology and mineral resources of Nigeria (Vol. 120): Springer.

Offodile, M.E., 2002, Groundwater Study and Development in Nigeria, Mecon Geology and Engineering Services Ltd, Jos, Nigeria.

Ofor, N.P. and Udensi, E.E., 2014, Determination of the Heat Flow in the Sokoto Basin, Nigeria using Spectral Analysis of Aeromagnetic Data. Journal of Natural Sciences Research, 4(6), 83-93.

Okubo, Y., Graf, J.R., Hansen, R.O., Ogawa, K. and Tsu, H., 1985, Curie point depth of the Island of Kyushu surrounding areas. Japan Geophysics, 53, 481-491.

Onuoha, K.M., Ofoegbu, C.O. and Ahmed, M.N., 1994, Spectral analysis of aeromagnetic data over the middle Benue trough, Nigeria. Journal of Mining and Geology, 30(2), 211-217.

Power Africa, 2018, Power Africa Nigeria Fact Sheet.

Rowland, A.A. and Ahmed, N., 2018, Determination of Curie Depth Isotherm and Geothermal Studies over Parts of Nasarawa and Environs, North Central Nigeria. International Journal of Energy and Environmental Science, 3(4), 69-81.

Salako, K.A., Adetona, A.A., Rafiu, A.A., Alahassan, U.D., Aliyu, A. and Adewumi, T., 2020, Assessment of Geothermal Potential of Parts of Middle Benue Trough, North-East Nigeria. Journal of the Earth and Space Physics, 45(4), 27-42.

Salako, K.A. and Udensi, E.E., 2013, Spectral depth analysis of parts of upper Benue trough and Borno basin, North-East Nigeria. Using Aeromagnetic Data. International Journal of Science and Research (IJSR), 2(8), 2319-7064.

Salem, A., Ushijima, K., Elsirafi, A. and Mizunaga, H., 2000, Spectral analysis of aeromagnetic data for geothermal reconnaissance of Quesir area, northern Red Sea. Proceedings of the World Geothermal Congress 2000, International Geothermal Association/IGA, 1669–1674.

Shehu, A.T., Olatunji, S. and Lawal, T.O., 2016, Assessment of Geothermal Potential of Sokoto Basin. Northwestern

Nigeria Using Spectral Centroid Analysis of High-Resolution Aeromagnetic (HRAM) Data. Journal of Science, Technology, Mathematics and Education, 12(2), 27-36.

Shuey, R.T., Schellinger, D.K., Tripp, A.C. and Alley, L.B., 1977, Curie depth determination from aeromagnetic spectra. Geophysical Journal Royal Astronomical Society, 50, 75–101.

Spector, A. and Grant, F., 1970, Statistical models for interpreting aeromagnetic data. Geophysics, 35(2), 293-302.

Stampolidis, A., Kane, I., Tsokas, G. and Tsourlos, P., 2005, Curie point depths of Albania inferred from ground total field magnetic data. Surveys in Geophysics, 26(4), 461-480.

Stacey, F.O., 1977, Physics of the Earth. John Wiley and sons. New York.

Tanaka, A., Okubo, Y. and Matsubayashi, O., 1999, Curie point depth based on spectrum analysis of the magnetic anomaly data in East and Southeast Asia. Tectonophysics, 306(3-4), 461-470.

Trifonova, P., Zhelev, Zh., Petrova, T. and Bojadgieva, K., 2006, Curie point depths of Bulgarian territory inferred from geomagnetic observations and its correlation with regional thermal structure

and seismicity. Tectonophysics, 473, 362–374.

Tselentis, G., 1991, An attempt to define Curie point depths in Greece from aeromagnetic and heat flow data. Pure and applied geophysics, 136(1), 87-101.

Ugwu, G.Z., Ezema, P.O. and Ezeh, C.C., 2013, Interpretation of Aeromagnetic data over Okigwe and Afikpo Areas of the Lower Benue Trough, Nigeria. International Research Journal of Geology and Mining (IRJGM), 3(1), 1-8.

Uysal, T., 2009, Tracing the Origin of Heat Anomalies in Hot Sedimentary Aquifer System in

Australia.   http://Geothermalenergy centreofExcellence.org.

Wright, J., Hastings, D., Jones, W. and Williams, H., 1985, Geology and Mineral Resources of West Africa. London: George Allen and Unwin publishers Ltd.

Zboril, L., 1984, Sketch map of oil-bearing structures. Geofyzika, Brno, Czechoslovakia. Pp. 94.

Zira, A.M., 2013, Challenges and Prospects of Geophysical Exploration of Geothermal System for National Development. Academic Journal of Interdisciplinary Studies, 2(12), 137-143.